JOURNAL OF GEOPHYSICAL RESEARCH, VOL. 95, NO. B13, PAGES 21,635-21,655, DECEMBER 10, 1990

HIGH-TEMPERATURE RAMAN SPECTROSCOPY OF SiO_2 AND GeO_2 POLYMORPHS: ANHARMONICITY AND THERMODYNAMIC PROPERTIES AT HIGH-TEMPERATURES

Philippe Gillet and Andrée Le Cléac'h

Laboratoire de Minéralogie Physique, Centre Armoricain d'Etude Structurale des Socles, Université de Rennes I, Rennes, France

Michel Madon

Département des Géomatériaux, Institut de Physique du Globe Paris, Paris, France

Abstract. The temperature dependence of the room pressure Raman spectra of the GeO_2 (hexagonal and tetragonal) and SiO_2 (quartz, coesite, and stishovite) polymorphs is presented. Several transformations upon heating are reported: α-β quartz, coesite-cristobalite, stishovite-silica glass (with Si in four-fold coordination). For all the compounds, Raman frequencies decrease linearly with temperature and the measured shifts are used in conjunction with available high-pressure Raman data to calculate for each compound intrinsic mode anharmonicity through the parameter $a_i=(\partial \ln \nu_i/\partial T)_V$. In quartz the modes related to the α-β transition (128 and 207 cm^{-1} modes) are highly anharmonic ($a_i=-20x10^{-5}\ K^{-1}$). In coesite many bands are unaffected by temperature and only two modes (77 and 116 cm^{-1}) show significant anharmonic behaviour. Tetragonal GeO_2 and stishovite behave similarly under temperature. Vibrational modeling of the specific heat and entropy, including anharmonic corrections deduced from the a_i parameters, are presented and compared to available calorimetric measurements. For the GeO_2 polymorphs the agreement between calculated and measured values is within 1-3% in the temperature range 100 to 1500 K. For quartz the agreement is similar over the range 50-850 K. For coesite and stishovite the models reproduce existing low temperature measurements. High-temperature values of C_p and entropy are proposed for coesite and stishovite.

1. Introduction

The phase changes occurring in SiO_2 are often the basis of pressure and temperature calibrations in piston-cylinder apparatus (quartz-coesite) or multi-anvil presses (coesite-stishovite). Moreover the change from four-fold (quartz and coesite) to six-fold coordination (stishovite) in silica is often called up to explain the 670 km seismic discontinuity. The SiO_2 polymorphs have been the subject of numerous experimental investigations: thermochemical measurements [Holm et al., 1967; Ghiorso et al, 1979; Richet et al., 1982; Akaogi and Navrotsky, 1984; Hemingway, 1987], elasticity measurements [Weidner and Carleton, 1977; Weidner et al., 1982], and vibrational modeling [Kieffer, 1979]. Despite the large variety of measurements, some inconsistencies remain, especially for the thermodynamic properties of coesite and stishovite. For instance, previous high-temperature (HT) extrapolations of C_p for coesite and stishovite show unusually high values compared to the C_p of quartz, cristobalite or SiO_2 liquid [Akaogi and Navrotsky, 1984]; see also discussion by Richet [1989].

Interest in the properties of GeO_2 mainly stems from the numerous structural and physical analogies with the SiO_2 system and especially from the common occurrence of isomorphous forms: hexagonal form (quartz structure) with Ge or Si in four-fold coordination, and tetragonal form with Ge or Si in six-fold coordination (rutile-type structure). Moreover, the GeO_2 polymorphs are stable at room pressure and thus readily amenable to various kind of physical and chemical measurements, including high-temperature calorimetric measurements [Richet, 1989] that cannot be performed for coesite or stishovite. Accurate measurements and modeling of the physical properties of the GeO_2 polymorphs may therefore provide useful information on the physical properties of the SiO_2 polymorphs.

Spectroscopic measurements (IR or Raman) are useful for estimating, via vibrational modeling, the thermodynamic properties of a mineral [Kieffer, 1979]. Such an approach also provides constraints on the thermodynamic properties of minerals at pressure and temperature conditions which cannot be reached by direct thermochemical measurements [Chopelas, 1990]. The pressure and temperature shifts of the optical vibrational modes can be suitably used to detect and measure mode anharmonicity, i.e., volume-driven effects versus intrinsic

Paper number 90JB01777.
0148-0227/90/90JB-01777$05.00

anharmonicity, as demonstrated on molecular crystals [Zallen and Slade, 1978] and tetragonal GeO_2 [Mammone and Sharma, 1979]. Intrinsic anharmonicity is a measure of the effect of temperature at constant volume on mode frequency; it is also a measure of the non parabolic shape of the interatomic potential. Gillet et al. [1989a] have introduced this measured mode anharmonicity in the vibrational modeling of the thermodynamic properties of olivine type compounds. Their model accounts for the observed departure from the harmonic limit of Dulong and Petit at high-temperature (HT) of the specific heat at constant volume.

M. Madon, Ph. Gillet, C. Julien and G.D. Price [Vibrational study of phase transitions among the GeO_2 polymorphs, submitted to Physics and Chemistry of Minerals, 1990] present a comprehensive high-pressure and high-temperature spectroscopic study (IR and Raman) of the GeO_2 polymorphs. This study shows that vibrational modeling accounts well for the measured properties of these polymorphs. Such an agreement is the starting point for using the same approach for the SiO_2 polymorphs.

Raman spectra of the SiO_2 (Qz, Cs, and St) and the GeO_2 (hexagonal end tetragonal) polymorphs are reported at temperatures up to 1300 K. They are compared with existing Raman and IR data. From these data and those obtained at high pressure [Hemley, 1987; Sharma, 1989; Madon et al., submitted manuscript 1990] we infer for each polymorph the anharmonicity of the observed Raman modes and we calculate the thermodynamic properties at HT, using the approach outlined by Gillet et al. [1989a]. Finally, we compare our results to available calorimetric data, and compare the analogical behavior of the SiO_2 and GeO_2 polymorphs and, we propose a new thermodynamic data set for the SiO_2 polymorphs.

2. Experimental procedures

Samples

We used powders of hexagonal GeO_2 provided by Prolabo. The tetragonal phase of GeO_2 was prepared by P. Richet (IPG Paris) by heating the hexagonal form at 1400 K for a period of several hours and subsequent quenching. Xray diffraction data showed that both products were single phases. Chips of quartz were cut from synthetic single crystals. Coesite and stishovite were kindly provided by J. Ingrin and F. Guyot, who synthesized these polymorphs at the Earth Science Department of the State University of New York at Stony Brook. The samples of these two polymorphs are polycrystalline, with a mean grain size of 1-20 μm.

Spectroscopy

Raman spectra were obtained on a Raman multichannel microprobe (Dilor microdil 28) at the Microsonde Laser Raman de l'Ouest service (Nantes University). High temperature Raman experiments were carried out by interfacing a heating stage (Leitz 1300) to the Raman microprobe [Gillet et al., 1988; Gillet et al., 1989a]. A chromel-alumel thermocouple was used for measuring temperature with an accurracy of ±1 K. The multichannel microprobe is equipped with an Olympus microscope. Leitz UTK40 and UTK50 objectives (focal distance 8 and 14 mm) were used. The excitation light, provided by the 514.5- or 488-nm lines of an Argon laser, is focused on the sample to a dimension as small as 1-2 μm. The Raman light is collected in the backscattering geometry and directed in the spectrograph equiped with 1800 gmm^{-1} grating. These gratings dispersed the signal to a multichannel detector which gives Raman windows of the order of 500 cm^{-1} in the 0-1500 cm^{-1} wave number region. Typical recording conditions were 20 accumulations of 30 s each, for 500 cm^{-1} wave number ranges. In order to observe a large number of bands, several grains with random orientations were studied. The output laser power was varied between 500-700 mW. Only 5-10% of this power reaches the sample, oving to absorption by the microscope objectives and spectrometer optics.

Absorption of the incident laser beam by the crystal may contribute to the sample heating and lead to phase transformation during the Raman scattering experiments. Such a phenomenon can be important for dark crystals. In order to check this possible heating we have recorded the Raman spectra of all the samples with various laser output powers (from 200 to 2000 mW). No shift or band broadening was observed, even for the 206 cm^{-1} Raman mode of quartz, which is very sensitive to temperature ($(\partial\nu_i/\partial T)$=-0.036 cm^{-1}/K). This implies that heating of the sample by the laser beam does not exceed 10-20 K. For stishovite no change in the Raman spectrum pattern was observed, even for very high laser output powers and long exposure time to the laser beam.

3. Results

Raman Spectra at Room Conditions

Quartz and hexagonal GeO_2 have the same irreducible representation of the optical vibrations:

$$\Gamma_{op} = 4A_1(R) + 4A_2(IR) + 8E(R+IR)$$

Measurements of the IR and Raman modes of quartz were made by Scott and Porto [1967]. Scott [1970] measured the Raman bands of hexagonal GeO_2 and noticed the striking similarities with quartz. Our room temperature spectra for both quartz and hexagonal GeO_2 are in excellent agreement with previous studies (Figures 1 and 2).

Coesite is monoclinic and the optical vibrations can be expressed as [Hemley, 1987]

$$\Gamma_{op} = 16A_g(R) + 17B_g(R) + 18A_u(IR) + 18B_u(IR)$$

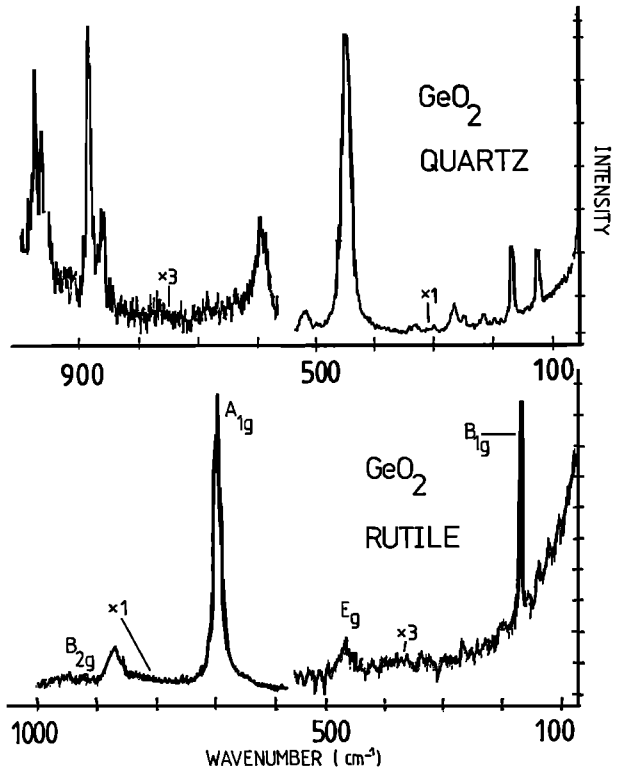

Fig. 1. Room pressure and temperature Raman spectra of the GeO_2 polymorphs.The numbers indicate the spectrum magnification.

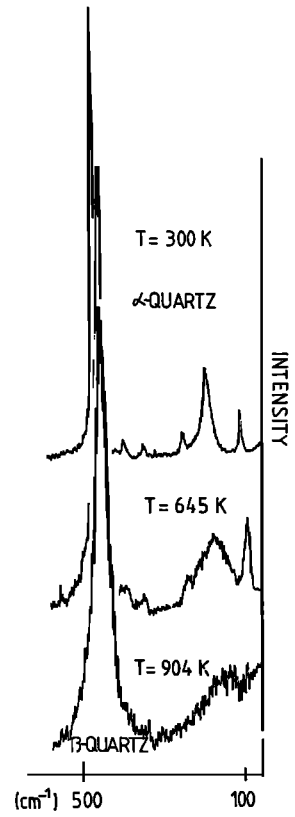

Fig. 2. Raman spectra of α-quartz at room pressure at 300, 645, and 904 K (β form). Only the spectra below 500 cm^{-1} are reported.

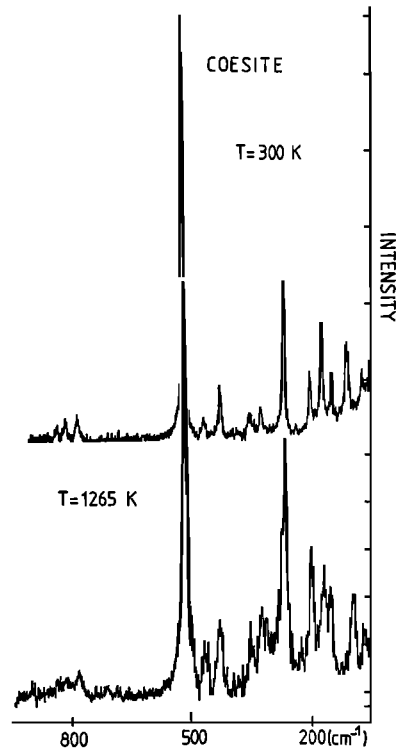

Fig. 3. Raman spectra of coesite at room pressure and at 300 and 1265 K.

Hemley (1987) has measured the Raman spectra of coesite at room pressure and up to 30 GPa. All bands he reported were observed in our sample (Figure 3). We have also observed two additional weak bands at 787 and 838 cm^{-1}.

Stishovite and tetragonal GeO_2 (rutile-type structure) have two formula units in the primitive cell and the irreducible representation [Dayal, 1950] :

$$\Gamma_{op} = A_{1g}(R)+A_{2g}(IR)+A_{2u}(IR)+B_{1g}(R) +B_{2g}(R)+2B_{1u}(IR)+E_g(R)+3E_u$$

The four Raman modes of stishovite were identified and assigned by Hemley et al. [1986] by comparison to those observed in other oxides having the ideal ordered rutile structure (e.g., GeO_2, TiO_2, SnO_2). Our Raman spectrum of stishovite is in excellent agreement (Figure 4) with the one he reported for synthetic stishovite. For tetragonal GeO_2 the three most intense lines (B_{1g}, 170 cm^{-1}; A_{1g}, 700 cm^{-1}; B_{2g}, 873 cm^{-1}) are in excellent agreement with previous works [Scott, 1970; Sharma, 1989] (Figure 1). The fourth expected band (E_g) has not been definitively observed. In some spectra a weak band at 465 cm^{-1} was observed. This weak band may arise from very small amounts of the hexagonal phase still present in the sample. However, the frequency of this mode lies at 20 cm^{-1} from the very intense 445 cm^{-1} mode of hexagonal GeO_2.

It is noted that natural stishovite from shocked sandstones exhibits a more complex Raman band pattern, different from the one expected for an ideal rutile structure [Nicol et al, 1980; Hemley et al., 1986]. In fact a previous spectrum of natural stishovite [Hemley et al., 1986]

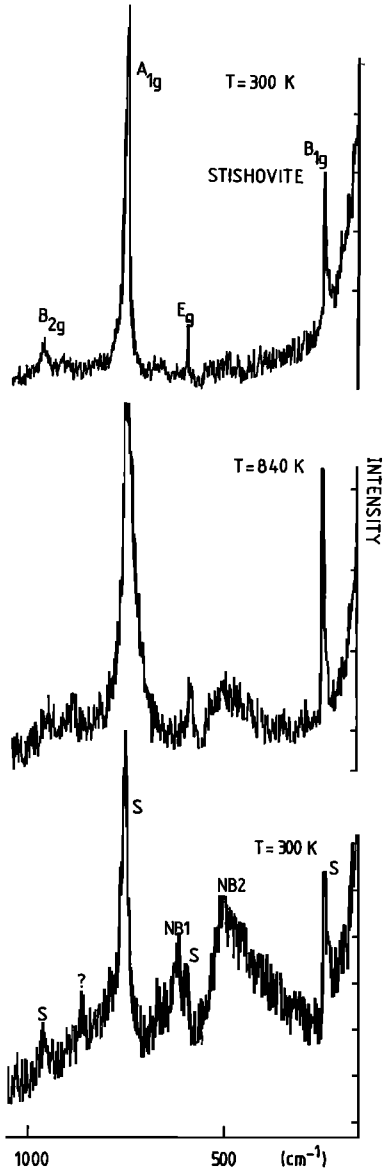

Fig. 4. Raman spectra of stishovite. The lower spectrum has been recorded on a sample heated at 800 K and subsequently quenched at room temperature. Note the new bands (NB1 and NB2) superimposed on those of perfect stishovite (S). NB1 and NB2 are characteristic of silica glass with Si in four-fold coordination.

shows additional bands, and especially a broad band (300-500 cm^{-1}). This broad band may indicate the presence of silica glass or may arise from multiphonon scattering due to structural disorder [Hemley et al., 1986]. We find evidences of similar phenomena in our heating experiments (discussed later).

High-Temperature Raman Results

Quartz. Fourteen Raman bands were monitored at temperatures up to the α/β transition at 846 K. Several heating experiments were conducted. Typical spectra are given in Figure 2. Most of the bands show a linear frequency decrease up to the α/ß transition (Figure 5). The temperature shifts at room temperature and pressure are reported in Table 1, along with data from previous works. Spectra collected at 904 K are characteristic of the ß phase (Figure 2) and are in excellent agreement with those reported by Bates and Quist [1972].

The measured shifts are in rather good agreement with those reported by Sharma [1989] with the exception of a few modes: we observe larger shifts for the 207 and 265 cm^{-1} modes. The frequency of the 207 cm^{-1} mode is rather difficult to follow because of large band broadening. However, Berge [1984] reported a similar large shift for this mode. For the 265 cm^{-1} the same shift was observed in different runs. The temperature-induced shifts of the IR modes (E modes: Raman and IR active) [Gervais and Piriou, 1975] seem to be greater than the corresponding Raman modes (Table1). But, since Gervais and Piriou [1975] do not report uncertainties in their data, further comparison cannot be made.

Hexagonal GeO_2. Heating of this phase is performed in the stability field of the tetragonal form which extents up to 1300 K at room pressure. The progressive transformation to the tetragonal form is observed during heating [Madon et al., submitted manuscript, 1990]. The strong A_g mode characteristic of tetragonal-modification starts to appear at around 1100 K (typical spectra are reported by Madon et al. [submitted manuscript, 1990]). Thirteen bands were tracked up to 1200 K (Figure 5). The temperature shifts are linear and in good agreement with those reported by Sharma [1989] (Table 3) with the exception of the 512 cm^{-1}, for which we have detected a more important shift. This mode is difficult to track because of considerable broadening of the 445 cm^{-1} band. However, it must be noticed that this band is also the most sensitive to pressure [Madon et al., submitted manuscript, 1990].

Some striking differences are found between the temperature-induced shifts in quartz and hexagonal GeO_2. The lattice instability of quartz is expressed by the existence of several modes (e.g., 207 and 128 cm^{-1}) having a large temperature shift, which is not observed in GeO_2. The mode at 517 cm^{-1} in GeO_2 representing Ge-O-Ge bends has a very important shift with temperature (-0.042 cm^{-1}/K). The main conclusion is that hexagonal GeO_2, as already noticed by Scott [1970], does not exhibit soft mode behavior.

Coesite. For coesite it was possible to measure the temperature dependence of 18 modes (Figure 3). Measurements were performed up to 1400 K for the modes lying below 550 cm^{-1} (LF modes), and up to 1150 K for the modes between 750 and 850 cm^{-1} (MF modes). Because of a poor signal to noise ratio, the high frequency bands (HF modes) (1000-1200 cm^{-1}) could only be followed up to 800 K. Temperature shifts are plotted in figure 6 and listed in Table 5. Most of the LF bands are unaffected by temperature increase, up to 900 K. Only four bands (77, 116, 177 and 521 cm^{-1}) show a continuous measurable linear decrease up to 1300 K. Four bands display a change at around 900 K. These bands are unaffected by temperature up to 900 K and show above

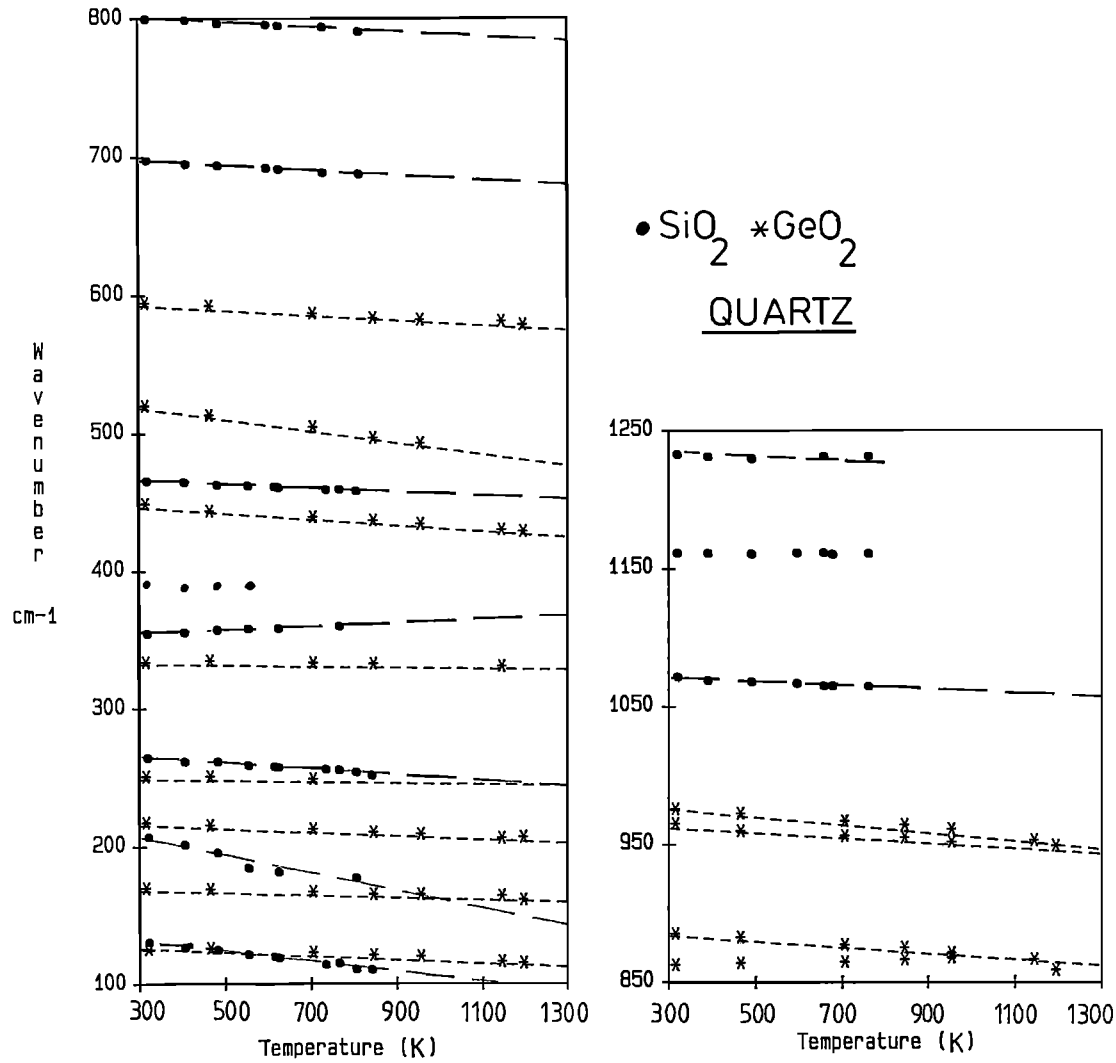

Fig. 5. Temperature dependence at room pressure of the Raman bands of quartz (dots) and hexagonal GeO_2 (stars). The error on frequency and temperature is less than the size of the plotting symbol.

this temperature small but measurable shifts or splittings (Figure 6). The MF and HF bands show a continuous linear decrease in frequency of the same order of magnitude as bands of similar wave numbers in quartz.

Heating up to 1400 K and recording of the spectra at several intermediate temperatures took on the order of 6 to 8 hours. During such an experiment the shifts are continuous (except the previously mentioned little changes at around 900 K) and the spectra at different temperatures are quite similar (except for the changes in frequency) to the spectrum recorded at room conditions. This indicates that the coesite structure is preserved over this temperature range for the run duration time.

Two longer duration experiments were carried out at temperatures between 1300-1400 K. These temperatures were reached in 2 hours. In a first run in which temperature was maintained at 1360 K (±5 K) for 2 hours, no changes in the Raman pattern could be detected in the several spectra recorded during this time interval. In a second run at 1400 K, a discontinuous non reversible change is observed after one hour of heating. The Raman spectrum after quenching reveals that coesite has broken down to cristabolite. No transformation of coesite to α or ß quartz was observed.

Stishovite. The weak B_{2g} mode could not be tracked as a function of temperature (Figure 4). The B_{1g} mode appears to be insensitive to temperature up to 1000 K. The frequencies of the other two modes decrease linearly with temperature (Figure 7). The measured shifts are reported in Table 8.

During progressive heating new features were observed in the Raman spectrum. Between 400-800 K, depending on heating time, the following changes were observed (Figure 4): (1) relative intensity change of the A_{1g} and B_{2g} modes, and (2) appearance of new bands; NB1 (600 cm^{-1}) and NB2 (broad diffuse and asymetric band peaking at around 480 cm^{-1}).

The new bands can coexist up to 1000 K with those characteristic of the rutile pattern. Raman spectra were also collected on quenched samples (Figure 4). All spectra showed the new bands but, depending on where the spectra were taken within the sample, the rutile bands

TABLE 1. Temperature Shifts of the Raman Modes of α-Quartz

Symmetry	ν_i, cm^{-1}	$(\partial\nu_i/\partial T)$,[a] cm^{-1}/K	$(\partial\nu_i/\partial T)$,[b] cm^{-1}/K	$(\partial\nu_i/\partial T)$,[c] cm^{-1}/K	$(\partial\nu_i/\partial T)$,[d] cm^{-1}/K
A_1	206	-0.065±0.005	-0.037		-0.065±0.005
	355	0±	+0.001		0
	464	-0.014±0.002	-0.014		
	1085	?	-0.015		
E(LO+TO)	128	-0.036±0.002	-0.033		
(LO+TO)	265	-0.022±0.002	-0.009		
(LO+TO)	696	-0.019±0.002	-0.013	-0.028	
(LO+TO)	1162	0	-0.006	-0.005	
E(TO)	394	+0.010±0.005	-0.006	+0.013	
(LO)	401	0	0	0	
(TO)	450	-0.020±0.005	+0.019	-0.038	
(LO)	511	?	?	-0.023	
(TO)	796	-0.019±0.003	-0.012	-0.028	
(LO)	808	-0.019±0.003	?	-0.026	
(TO)	1069	-0.015±0.002	-0.014	-0.013	
(TO)	1230	-0.006±0.002	-0.006	0	

[a]This work.
[b]Data from Sharma (1989).
[c]Data from Gervais and Piriou (1975).
[d]Data from Berge (1984).

TABLE 2. Mode Gruneisen and Anharmonic Parameters of α-Quartz

ν_i, cm^{-1}	γ_{iP}°[a]	γ_{iT}°[b]	a_i°,[c] $10^{-5}K^{-1}$	γ_{iP},[d]	γ_{iT},[e]	a_i,[f] $10^{-5}K^{-1}$	a_i,[g] $10^{-5}K^{-1}$
206	9.0±1.2	3.58±0.08	-19.0±3.0	8.3	3.3	-22.9	-2.4
356	0.0±0.06	-0.13±0.04	-0.5±0.1	0.0	-0.01	-0.4	0.7
464	0.9±0.2	0.64±0.02	-0.8±0.2	0.7	0.5	-0.8	-1.5
1085	?	0.05±0.01	?	?	?	?	-1.2
128	8.0±0.9	1.65±0.08	-22.3±3.7	7.3	1.4	-26.5	-20.2
265	2.4±0.4	0.49±0.01	-6.6±1.1	1.9	0.4	-6.9	-0.4
696	0.8±0.1	0.37±0.03	-1.4±0.4	0.6	0.3	-1.5	-0.5
1162	0.0±0.06	-0.10±0.01	-0.4±0.1	0.0	-0.08	-0.3	-0.4
394	-0.7±0.4	-0.01±0.003	2.50±2	-0.6	-0.006	2.5	-1.55
401	0.0±0.06	-0.01±0.003	-0.03±0.01	0.0	-0.006	-0.03	-0.05
450	1.3±0.4	0.38±0.01	-3.10±1.1	1.0	0.3	-3.2	-2.8
511	?	0.38±0.01	-3.10±1.1	?	0.3	-3.2	?
796	0.7±0.1	0.27±0.03	-1.4±0.5	0.5	0.2	-1.4	?
808	0.7±0.14	0.27±0.03	-1.4±0.5	0.5	0.2	-1.4	-0.6
1069	0.4±0.08	0.04±0.003	-1.3±0.3	0.3	0.03	-1.3	-1.15
1230	0.14±0.08	0.04±0.003	-0.3±0.2	0.1	0.03	-0.4	-0.9

[a]Calculated from the present temperature shifts and $\alpha_0=3.5\times10^{-5}$ K^{-1} [Ghiorso et al., 1979].
[b]Data from Hemley (1987).
[c]Calculated from $a_i=\alpha_0(\gamma_{iT}-\gamma_{iP})$.
[d]Calculated at 800 K with the actual values of ν_i at 800 K and $\alpha_{800}=4.55\times10^{-5}$ K^{-1} [Ghiorso et al., 1979].
[e]Calculated with ν_i at 800 K and K_{800}=28.3 GPa [Ghiorso et al., 1979].
[f]Calculated with data of preceding columns and $\alpha_{800}=4.55\ 10^{-5}\ K^{-1}$.
[g]Data from Sharma [1989].

TABLE 3. Temperature and Pressure Shifts of the Raman Modes of Hexagonal GeO_2

Symmetry.	ν_i cm^{-1}	$(\partial\nu_i/\partial T)$,[a] cm^{-1}/K	$(\partial\nu_i/\partial T)$,[b] cm^{-1}/K	$(\partial\nu_i/\partial P)$,[c] cm^{-1}/GPa	$(\partial\nu_i/\partial P)$,[b] cm^{-1}/GPa
A_1	212	-0.011±0.002	-0.008	4.3±0.3	5.0
	261	-0.015±0.003	-0.008	6.2±0.3	5.6
	442	-0.019±0.002	-0.019	9.1±0.4	8.6
	880	-0.025±0.4	-0.025	0	2.2
E(LO+TO)	122	-0.009±0.001	-0.008	3.1±0.5	3.7
(LO+TO)	164	-0.008±0.001	-0.008	0.95±0.10	1.2
E(TO)	327	+0.005±0.002	-0.008	2.1±0.3	1.9
(LO)	372	?	?	?	?
(TO)	385	?	?	?	?
(LO)	456	?	?	?	?
(TO)	492	?	?	?	?
(LO)	514	-0.042±0.005	-0.027	10.8±0.5	11.9
(TO)	583	-0.022±0.003	-0.024	9.1±0.5	8.2
(LO)	595	-0.022±0.003	-0.024	9.1±0.5	8.2
(TO)	857	-0.015±0.002	-0.018	0	-0.7
(LO)	949	?	?	?	?
(TO)	961	-0.025±0.003	-0.028	1.0±0.5	-8
(LO)	970	-0.023±0.003	-0.023	0	0

[a]This work.
[b]Data from Sharma [1989].
[c]Data from Madon et al. [submitted manuscript, 1990].

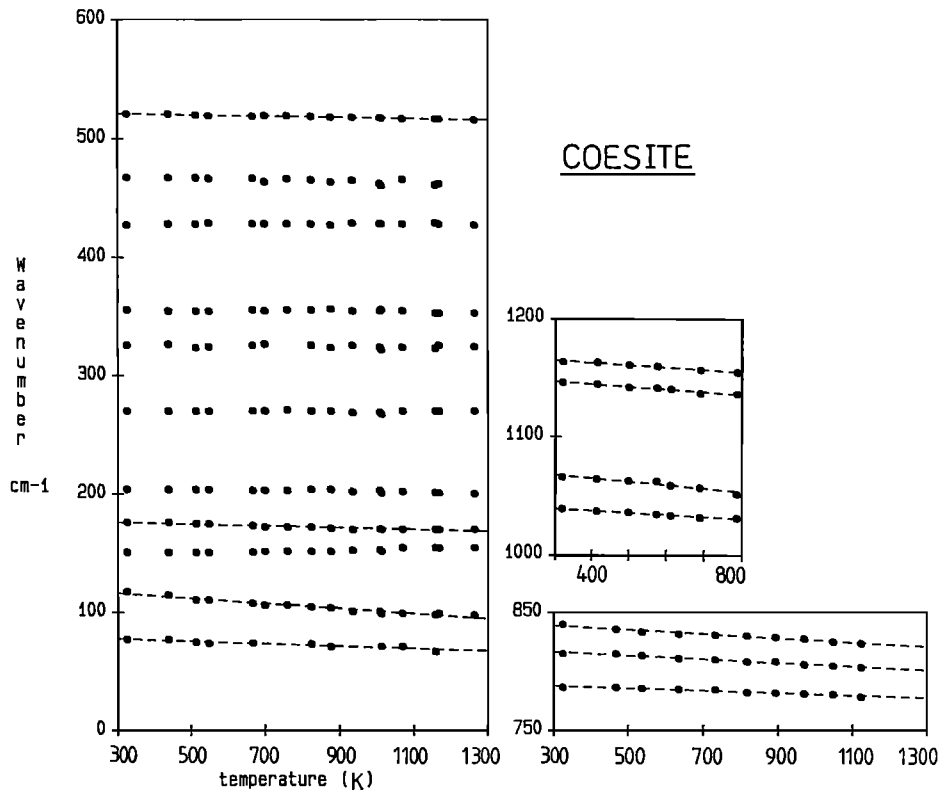

Fig. 6. Temperature dependence at room pressure of the Raman bands of coesite. Note that all the bands between 200 and 500 cm^{-1} are unaffected by temperature.

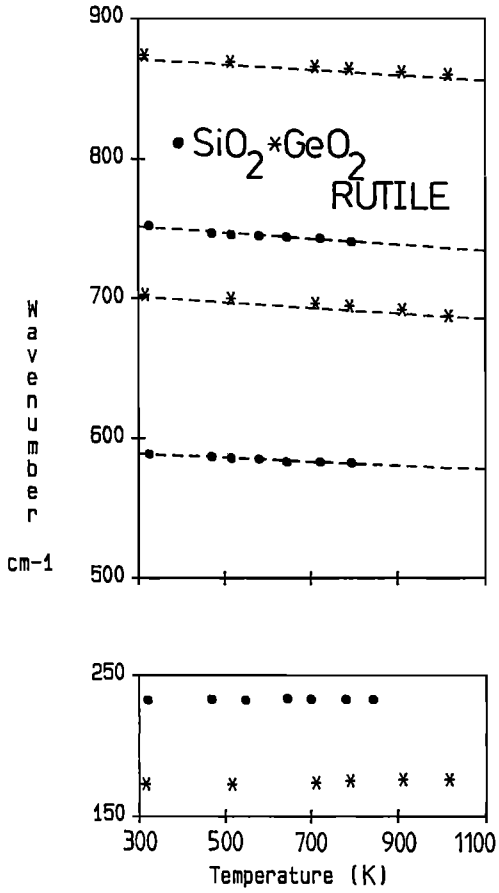

Fig. 7. Temperature dependence at room pressure of the Raman bands of tetragonal GeO_2 and stishovite. Dots are for SiO_2 and stars for GeO_2.

were not always observed. The intensity of NB1 and NB2 relative to rutile bands varies from place to place within the sample.

Observation of the sample by transmission electron microscopy (TEM) reveals the coexistence of stishovite with a SiO_2 glassy phase. The size of the glass domains varies and is less than 1 μm. The features observed by Raman spectroscopy can therefore be explained by the progressive and incomplete transformation of stishovite during heating. Moreover, our data suggest that stishovite inverts directly to silica glass with Si in fourfold coordination. In fact the NB1 and NB2 bands are characteristic of silica glass [Sharma et al., 1981]. The present observations confirm the experimental results of Skinner and Fahley [1963] and the theoretical predictions of Richet [1988]. Heating and transformation induced by the laser beam have been ruled out (see section 2). Moreover heated samples on which the laser beam has not been focused reveal the same textures.

Some spectra collected at HT or on quenched samples show striking analogies with the Raman spectrum of natural stishovite reported by Hemley et al. [1986]. The broad bands observed in the natural samples can be assigned to the presence of small amounts of silica glass. Such an interpretation is supported by the TEM observations of Werner-Kieffer [1976] on the same samples. In fact, as in our heated samples, natural stishovite is interwoven with glass at a scale less than 0.5 μm, i.e., at a size smaller than the 1 μm diameter of the laser spot of the Raman probe. Our new observations seem to rule out the assignment of the extra bands as second order Raman bands due to disordering effects [Nicol et al., 1980; Hemley et al., 1986)]. The exact temperature of the stishovite to glass transition could not be evaluated because the transformation is time-dependent [Skinner and Fahley, 1963)]. More recently, IR data on both natural and synthetic stishovite have also shown spectral differences which have been attributed (or best explained) as $(SiF_6)^{2-}$ impurities and not to SiO_2 glass impurities [Hofmeister et al., 1990].

Tetragonal GeO_2. The B_{1g} mode exhibit a slight frequency increase with temperature as already reported by Sharma [1989] (Figure 7). The E_g mode mode could not be monitored and the two remaining modes (A_{1g} and B_{2g}) see their frequency decreasing with temperature (Figure 7 and Table 6). Our results are in fairly good agreement with those of Sharma [1989].

4. Anharmonicity

Mode anharmonicity

The temperature and pressure dependence of a given vibrational mode (of frequency ν_i) arises from two contributions: (1) a pure-volume contribution due to compressibility and thermal expansion and, (2) a volume independent (pure temperature) contribution arising from higher-order anharmonic interactions.

Gillet et al. [1989a], following previous works [Peercy and Morosin, 1973; Mammone and Sharma, 1979; Zallen and Slade, 1978], have used a mode anharmonic parameter for discussing crystal anharmonicity:

$$a_i=\left(\frac{\partial \ln \nu_i}{\partial T}\right)_V$$

The mode parameter a_i corresponds to an intrinsic anharmonic parameter. It is also an intrinsic derivative in accordance with the definition of Anderson [1988]. It expresses a change in frequency due to temperature at constant volume. Gillet et al. [1989a] have shown that

$$a_i=\alpha(\gamma_{iT}-\gamma_{iP})$$

with

$$\gamma_{iT}=K\left(\frac{\partial \ln \nu_i}{\partial P}\right)$$

$$\gamma_{iP}=\frac{1}{\alpha}\left(\frac{\partial \ln \nu_i}{\partial T}\right)$$

where α is the coefficient of thermal expansion, K is the bulk modulus, γ_{iT} is the classical mode Gruneisen

parameter, and γ_{iP} is similar to the elastic Anderson-Gruneisen parameter. In the pure harmonic approximation $a_i=\gamma_{iT}=\gamma_{iP}=0$. In the quasi-harmonic approximation the bands behave harmonically, but their equilibrium length can change and we have thus $a_i=0$ and $\gamma_{iT}=\gamma_{iP}$. In the quasi-harmonic approximation the parameters γ_{iT} and γ_{iP} bear the same information. In a true anharmonic case the above parameters are not equal. The anharmonic parameter a_i can be deduced from the measurements of frequency versus temperature and versus pressure and from α and K.

The a_i, γ_{iT} and γ_{iP} parameters are temperature-dependent because α, K, and ν_i are known functions of temperature. Let us examine the uncertainties in all the terms involved in the calculation of a_i and the variation of a_i with temperature. A detailed discussion can be made for quartz for which a rather complete data set is available. Superscripts and subscripts 0 refer to parameters values at 300 K and 0.1 MPa.

Quartz. The γ_{iP} are only sensitive to the uncertainties in α_0 and slopes of the frequency versus temperature curves. The values of γ_{iP} and their related uncertainties were calculated with $\alpha_0=3.5\pm0.2\times10^{-5}$ K^{-1} [Skinner, 1966; Ghiorso et al, 1979] and the measured shifts and related uncertainties of the present study (Table 2). The a_i parameters were derived from our γ_{iP} and the γ_{iT} and related uncertainties reported by Hemley [1987] (Table 2). With the exception of the 394 cm^{-1} mode (which presents large uncertainties) all the a_i parameters are negative and significantly different from zero. This implies that the frequency changes are not driven by volume changes alone.

The effect of temperature on a_i can be estimated only qualitatively. Because $(\partial\nu_i/\partial T)$ is constant up to α-β transition, the evolution of γ_{iP} depends only on the actual values of α and ν_i at a given temperature. The calculations performed at 800 K show that the γ_{iP} values slightly decrease with temperature (Table 2). The calculation of γ_{iT} at different temperature is less easy. The parameters K and ν_i decrease with temperature but the main unknown concerns the variation of $(\partial\nu_i/\partial P)$ with temperature. The pressure shifts measured at 4 K [Briggs and Ramdas, 1977] do not significantly differ from those of Hemley [1987], Dean et al. [1982] and Asell and Nicol [1968] at 300 K. This result does not rule out a possible change in $(\partial\nu_i/\partial P)$ at higher temperatures, as suggested by the data of Dietrich and Arndt [1982] on forsterite. We have calculated γ_{iT} at 800 K with the actual value of K and ν_i at this temperature and by assuming $(\partial\nu_i/\partial P)$ to be independent of T; this calculation provides only upper limits for the γ_{iT}. The γ_{iT} are slightly decreasing with temperature (Table 2). The a_i parameters at 800 K (Table 2) are slightly smaller than at 300 K but, taking into account all the uncertainties involved in the calculation, they can be considered as constant from 300 to 800 K. At the vicinity of the α–β transition, $(\partial\nu_i/\partial T)$ of certain modes and α may drastically change and lead to significant changes in the a_i. If one excepts the 206 and 265 cm^{-1} modes the present data for the a_i are of the same sign and order of magnitude as those reported by Sharma [1989].

The 128 and 207 cm^{-1} modes are highly anharmonic reflecting their important instability. Finally, it must be noticed that modes having an anomalous behavior under pressure (frequency decrease with pressure) also have an anomalous behavior under temperature (frequency increase with temperature or unaffected by temperature).

For the other compounds, it will assumed that the values of the a_i are also nearly constant with temperature and close to those calculated at room temperature.

Hexagonal GeO_2. The γ_{iT} and their uncertainties are taken from Madon et al. [submitted manuscript, 1990]; they are very close to the values reported by Sharma [1989] (Tables 3 and 4). The γ_{iP} parameters were calculated from the present temperature shifts and related uncertainties and two extreme values of α_0 taken from Murthy [1962] and M. Okuno and I. Minato (personal communication, 1990) (Table 4). The a_i parameters are negative and are all of the same order of magnitude with the exception of the 517 cm^{-1} mode (Table 4), in contrast to what has been observed in quartz.

Coesite. In many ionic compounds, structural parameters are primarily a function of molar volume. Structural variations with increasing pressure or decreasing temperature are similar. This inverse relationship between the pressure and the temperature response of a solid is also generally qualitatively true for the mode frequencies. For most of the Raman modes observed in coesite this inverse relationship holds (Table 5). There are three frequency regions with similar pressure and temperature behavior. From 77 to 176 cm^{-1} the modes are sensitive to both pressure and temperature and the a_i parameters are large and negative. From 204 to 466 cm^{-1} the modes are less sensitive to pressure and are not affected by temperature. In this region the a_i parameters are positive and close to 0. From 551 to 1164 cm^{-1} the modes are more sensitive to temperature than to pressure; the a_i parameters are higher and negative. Such a behavior must be related to structural variation (bond length and bond angle variations) of coesite under pressure and temperature. Hemley [1987] has related the behavior of the Raman modes under pressure with available data on bond length and bond angle variations with pressure. Such a comparison cannot be made for the present data because HT Xray measurements are lacking.

Stishovite and Tetragonal GeO_2. The γ_{iT}, γ_{iP} and a_i parameters have been calculated with their uncertainties using different values of α_0 (Tables 7 and 9). The Raman modes characteristic of the rutile structure have quite similar values in both GeO_2 and SiO_2. Such similarities indicate that tetragonal GeO_2 is a good analogue of stishovite. The B_{1g} mode has a negative pressure dependence and either no or a small positive temperature dependence. The other modes follow the inverse relationship observed for most of the modes in quartz and coesite. The data show that even if little mode anharmonicity is observed for the lowest Raman mode, the self-energy shifts of the other modes are dominated by the pure volume term due to thermal expansion.

The anisotropic compression of stishovite (the a axis being 50 % more compressible than the c axis) is reflected in the behavior of the Raman modes with pressure

TABLE 4. Mode Gruneisen and Anharmonic Parameters of Hexa-GeO_2.

ν_i cm^{-1}	γ_{iP}[a]	γ_{iP}[b]	γ_{iP}[c]	γ_{iT}[d]	a_i,[e] $10^{-5}K^{-1}$	a_i,[f] $10^{-5}K^{-1}$
212	1.73	2.23	2.0±0.2	0.8±0.05	-3.1±0.8	-2.5
261	1.92	2.47	2.2±0.2	0.9±0.05	-1.3±0.3	-0.5
442	1.44	1.84	1.6±0.2	0.8±0.03	-2.1±0.6	-2.1
880	0.95	1.22	1.1±0.2	0	-2.9±0.7	-2.6
122	2.47	3.17	2.8±0.2	0.9±0.2	-3.8±1.3	-2.5
164	1.63	2.09	1.8±0.2	0.2±0.02	-4.1±1.2	-4.2
327	0.51	0.65	0.6±0.1	0.2±0.03	-0.9±0.3	-1.7
514	2.74	3.51	3.1±0.2	0.8±0.05	-5.9±1.3	-2.7
583	1.26	1.62	1.4±0.2	0.6±0.03	-2.1±0.6	-2.5
595	1.23	1.58	1.4±0.2	0.6±0.03	-2.1±0.6	?
857	0.58	0.75	0.6±0.2	0	-1.6±0.5	-2.2
961	0.87	1.12	1.0±0.1	0.04±0.02	-2.5±1.7	-4
970	0.79	1.02	0.9±0.1	0	-2.3±0.7	-2.2

[a]Calculated from the present temperature shifts and $\alpha_0=2.99.10^{-5}$ K^{-1} [Murthy, 1962].
[b]Same as preceding column but with $\alpha_0=2.33x10^{-5}$ K^{-1} (M. Okuno and I. Minato, personal communication, 1990).
[c]Mean values between preceding two columns.
[d]Data from Madon et al. [submitted manuscript, 1990].
[e]Calculated with preceding two columns and $\alpha_0=2.6\pm0.3x10^{-5}$ K^{-1}.
[f]Data from Sharma [1989].

TABLE 5. Temperature Shifts, Mode Gruneisen and Anharmonic Parameters of Coesite

ν_i cm^{-1}	$(\partial\nu_i/\partial T)$,[a] cm^{-1}/K	γ_{iP}[b]	γ_{iT}[c]	a_i,[d] $10^{-5}K^{-1}$
77	-0.01±0.001	17.3±5.2	2.7±0.3	-10.9±6.7
116	-0.021±0.002	24.1±7.2	6.1±0.4	-13.7±7.7
151	0	0	0.5±0.1	0.4±0.15
176	-0.008±0.001	6.1±1.1	3.0±0.1	-2.3±1.0
204	0	0	1.1±0.1	0.80±0.2
269	0	0	0.4±0.08	0.30±0.1
326	0	0	0.3±0.05	0.20±0.08
355	0	0	0.12±0.01	0.10±0.02
427	0	0	0.1±0.01	0.08±0.02
466	0	0	0.14±0.01	0.10±0.03
521	-0.005±0.001	1.3±0.4	0.53±0.02	-0.50±0.2
661	?	?	0.90±0.06	?
787	-0.011±0.001	1.9±0.5	?	?
795	?	?	0.27±0.02	?
815	-0.016±0.001	2.6±0.8	0.61±0.03	-1.50±0.6
838	-0.019±0.002	3.0±0.9	?	?
1036	-0.016±0.001	2.1±0.6	0.02±0.01	-1.50±1.0
1065	-0.028±0.002	3.5±1.0	-0.12±0.01	-2.70±1.6
1144	-0.021±0.001	2.4±0.7	0.14±0.03	-1.70±0.8
1164	-0.019±0.002	2.2±0.6	0.13±0.02	-1.50±0.8

[a]Data from this work.
[b]Calculated from the present temperature shifts and $\alpha_0=0.75\pm0.15x10^{-5}$ K^{-1} [Skinner, 1966].
[c]Data from Hemley [1987].
[d]Calculated from preceding two columns and $\alpha_0=0.75\pm0.15x10^{-5}$ K^{-1}.

TABLE 6. Temperature shifts the Raman modes of tetragonal GeO_2

Sym.	ν_i,cm^{-1}	$(\partial\nu_i/\partial T)$, cm^{-1}/K	
		This Work	Sharma [1989]
B_{1g}	170	0.003±0.001	0.004
A_{1g}	700	-0.022±0.002	-0.022
B_{2g}	873	-0.019±0.002	-0.026

[Hemley, 1987]. Raman modes with motions along the c axis (E_g modes) have smaller pressure shifts relative to those modes with displacements perpendicular to c (A_{1g} modes). In contrast the B_{1g} mode has a negative pressure dependence. Our high-temperature data show that E_g modes have smaller temperature shifts relative to the A_{1g} modes. This is also reflected by the strong anisotropy in thermal expansion of stishovite, the a axis being more expansible than the c axis [Ito et al., 1974; Endo et al., 1986].

Discussion

The relative anharmonicity of the SiO_2 polymorphs can be discussed at the level of individual modes or by taking average values of a_i over the observed modes. There are evidences of the types of atomic motions associated with observed bands in quartz from comparative studies of spectra and lattice dynamics calculations (see for instance, McMillan and Hess [1990]). The high-frequency modes (>500 cm^{-1}) have large contributions from Si-O stretching motions and the low-frequency modes involve complex translations and rotations of the SiO_4 tetrahedra. It is expected that similar contributions occur in coesite where Si is also in four-fold coordination. In stishovite where Si is in six-fold coordination. Hemley et al. [1986] has suggested that the modes between 750 and 1000 cm^{-1} are due to SiO_6 asymetric stretches and those lying between 700 and 500 cm^{-1} are predominantly due to SiO_6 stretches and bends.

For quartz and coesite the high-frequency modes related to Si-O stretches have similar relatively low a_i values and the lowest Raman modes show a more pronounced anharmonic behavior. There is no clear relationship between the value of the a_i and wave number. Such a behaviour has also been observed in forsterite [Gillet et al.,1989b]. The mean value $\langle a_i \rangle$ is higher in quartz than in coesite (-3.94 and -1.86x10^{-5}, respectively). For stishovite it seems also that the high-frequency modes are less anharmonic than the low-frequency modes, but the difference is less pronounced than in quartz or coesite. We also note that modes related to Si-O stretches have the same degree of anharmonicity when Si is in four-fold or six-fold coordination. The $\langle a_i \rangle$ value of stishovite is -1.53x10^{-5}. Our data suggest so far that from a spectroscopic point of view, anharmonicity (measured by $\langle a_i \rangle$) seems to decrease when going through the quartz-coesite and coesite-stishovite transformations. This result is at variance with the conclusions of Jeanloz and Roufosse [1982]. Our results must be considered with caution in the absence of complete measurements (especially for stishovite) of infrared-active modes under pressure and temperature. We suggest therefore that the $\langle a_i \rangle$ of a mineral can be used to measure its degree of anharmonicity.

5. Thermodynamic Modeling

Most of the existing data (see Akaogi and Navrotsky [1984], Kuskov and Fabrichnaya [1987] and Fei et al. [1990] for reviews) concerning the thermodynamic properties of the SiO_2 polymorphs indicate many discrepancies which might lie in the single determination of the thermochemical data of coesite and stishovite [Holm et al., 1967]. Therefore, we reexamine these data and provide, using vibrational modeling, a new set of C_p and entropy values for coesite and stishovite up to 1500 K.

Madon et al. [submitted manuscript, 1990] present a high-pressure and high-temperature spectroscopic (IR and

TABLE 7. Mode Gruneisen and Anharmonic Parameters of Tetragonal GeO_2

Sym.	ν_i, cm^{-1}	γ_{iP}[a]	γ_{iP}[b]	γ_{iP}[c]	γ_{iT}[d]	a_i,[e] 10^{-5} K^{-1}
B_{1g}	170	-0.87	-1.33	-1.1±0.5	-2.8±0.4	-2.7±2.2
A_{1g}	700	1.55	2.36	1.9±0.5	1.4±0.2	-0.9±0.5
B_{2g}	873	1.07	1.63	1.4±0.4	1.3±0.2	-0.01±0.006

[a]Calculated from the present temperature shifts and α_0=2.03x10^{-5} K^{-1} [Rao et al., 1968].
[b]Same as preceding column but with α_0=1.33 10^{-5}xK^{-1} (M. Okuno and I. Minato, pers. com., 1990).
[c]Calculated from the present temperature shifts and related experimental uncertainties and α_0=1.6±0.3x10^{-5} K^{-1}.
[d]Data from Sharma [1989].
[e]Calculated with preceding two columns and α_0=1.6±0.3x10^{-5} K^{-1}.

TABLE 8. Temperature Shifts of the Raman Modes of Stishovite

Sym.	ν_i,cm^{-1}	$(\partial\nu_i/\partial T)$, cm^{-1}/K
B_{1g}	231	0.0±0.001
E_g	589	-0.014±0.001
A_{1g}	753	-0.022±0.002

Raman) study of the hexagonal and tetragonal forms of GeO_2 together with a vibrational modeling of C_p and S. For the GeO_2 polymorphs a comprehensive set of measured S and Cp data from 0 to 1500 K is available [King, 1958; Counsell and Martin, 1967; Richet, 1989], allowing a comparison between calculated and measured values. The excellent agreement between the two approaches in the case of the GeO_2 polymorphs provides the starting point for the computation of C_p and S for the SiO_2 polymorphs, and especially for stishovite and coesite, for which high-temperature measurements are lacking owing to transformation during heating.

Vibrational Modeling

The starting model we use is that of Kieffer [1979]. Her model [see Akaogi et al., 1984; Hofmeister, 1987] predicts the quasi-harmonic specific heat at constant volume (C_v) and the quasi-harmonic entropy S at temperatures up to 1000 K. The vibrational density of states used in the calculations is derived from available spectroscopic data (IR and Raman) and from measured acoustic velocities. In the model, the vibrational density of states is divided in two contributions: (1) three acoustic modes assumed to be Debye-like; (2) the remaining modes (optically active or inactive), which are treated as optic continua, a constant density of states between a low- and a high-frequency cutoff, in which the modes are uniformly distributed. The number of continua and their cutoffs are inferred from IR and Raman data, mode denumbering and assignments of modes to specific vibrations [see Hofmeister [1987] and Chopelas [1990] for improvements of Kieffer's model with several optic continua). However, whatever the degree of model refinement the quasi-harmonic assumptions (i.e. a_i=0) underlying the model imply that C_V always tends toward the Dulong and Petit limit at HT.

Model uncertainties. Previous studies on silicates or their analogues for which calorimetric data can be compared with calculated values, have shown that model uncertainties must be discussed in two distinct temperature ranges.

Between 0 and 300 K, C_v and particularly S are very sensitive to details of the density of states of the optical modes. The number of modes below 300 cm^{-1} and the frequency of the lowest optic mode are crucial model parameters. Below 300 K it can be assumed that C_v=C_p, the corrective term α^2VKT being negligible, and measured values of C_p and S can be directly compared to calculated C_v and S.

Above 300 K, different models consistent with the spectroscopic data show that C_v and S are less sensitive to details of the density of states. The major uncertainties come from the α^2VKT term, when converting C_v to C_p, and also from anharmonic effects on C_v which may become important above 1000 K. Thus the conversion of C_v to C_p must be carried out with different high-temperature extrapolations of α and K in order to bracket the α^2VKT term at high temperatures. It will be shown in the following discussion that anharmonic effects on C_v can be included in Kieffer's model using the previously measured a_i parameters.

Moreover, insights on the high-temperature thermodynamic properties of a silicate, for which measurements are lacking, can be inferred from a study on an analogue (same structure but different chemistry) for which termodynamic measurements are available. A model of the density of states, compatible with measured thermodynamic quantities, can be transferred to the silicate compound. We will adopt this approach for stishovite.

Anharmonic correction to C_v. Gillet et al. [1989a] have shown on Ca_2GeO_4 olivine that at temperatures greater than 1000 K, the harmonic assumptions of Kieffer's model are no longer valid and proposed a way to introduce anharmonic corrective terms in this model. In a forthcoming paper [Gillet et al., manuscript in preparation]

TABLE 9. Mode Gruneisen and Anharmonic Parameters of Stishovite

Sym.	ν_i,cm^{-1}	γ_{iP}[a]	γ_{iP}[b]	γ_{iP}[c]	γ_{iT}[d]	a_i,[e] 10^{-5} K^{-1}
B_{1g}	231	0.0	0.0	0.0±0.1	-1.58±0.06	-2.5±0.5
E_g	589	1.67	1.28	1.5±0.4	1.0±0.03	-1.4±0.6
A_{1g}	753	2.06	1.57	1.8±0.5	1.38±0.042	-0.7±0.3

[a]Calculated from the present temperature shifts and α_0=1.42x10^{-5} K^{-1} [Ito et al., 1974].

[b]Same as preceding column but with α_0=1.86 10^{-5} K^{-1} [Endo et al.,1986].

[c]Calculated from the present temperature shifts and related experimental uncertainties and α_0=1.6±0.3 10^{-5} K^{-1}.

[d]Data from Hemley [1987)].

[e]Calculated with preceding two columns and α_0=1.6±0.3x10^{-5} K^{-1}.

TABLE 10. Input Data Used in Vibrational Modeling and for Converting C_V to C_p

Compound	u_1, m/s	u_2, m/s	u_3, m/s	V_0, cm^3/mol	α, $10^{-5}K^{-1}$	K, GPa
GeO_2 hex.	4100[a]	2550	2550	24.39[b]	2.99+1.07x10^{-3}(T-300)[c] 2.2+5x10^{-4}T[e]	39.1[d]
GeO_2 tetr.	8500[f]	4700	4700	16.66[b]	1.11+7x10^{-4}T[e] 2.03+2x10^{-3}(T-300)[g]	265[g]
Quartz	6020[i]	4460	3760	22.69[b]	3.5+5.26x10^{-3}(T-273)[j] -2.43x10^{-5}(T-273)^2 +8.22x10^{-8}(T-273)^3	37.4[d]
Coesite	8190[i]	5240	4170	20.64[b]	0.54+0.83x10^{-3}T[k] 0.57+0.75x10^{-3}T[m]	96[e]
Stishovite	11000[i]	6190	5050	14.06[b]	1.012+1.35x10^{-3}T[k] 1.48+8.1x10^{-4}T[m]	306[n]

[a]Soga [1971].
[b]Robie et al. [1982].
[c]Murthy [1962].
[d]McSkimmin et al. [1965].
[e]M. Okuno and I. Minato (personal communication, 1990).
[f]Striefler and Barsch [1976].
[g]Lieberman [1973]
[h]Rao et al. [1968].
[i]Kieffer [1979].
[j]Ghiorso et al. [1979)].
[k]Fei et al. [1990].
[l]Lieven and Prewitt [1981].
[m]Duffy and Anderson [1989].
[n]Weidner et al. [1982].

we show , in the case of forsterite, that such anharmonic effects are important and present the complete way of calculating them. Only a brief discussion is presented here. We will focus on the effect of anharmonicity on C_V only for the optic modes, because the acoustic modes, even if they are anharmonic only contribute to C_V at low temperatures where anharmonic effects are negligible.

In Kieffer's model the contribution to C_V of m optic continua is given by

$$C_v=3nR\sum_{i=1}^{m}\int_{v_{li}}^{v_{ui}}\frac{x^2\exp(x)dv}{(v_{ui}-v_{ul})(\exp(x)-1)^2}$$

$$C_v=3nR\sum_{i=1}^{m}C_{vhi}$$

where $x = (hv_i/kT)$
n : number of atoms in the mineral's formula.
R : gas constant.
N : the total number of vibrations.
v_{li} (v_{ui}) : the lower (upper) cutoffs frequencies of the ith continuum
C_{vhi} : harmonic contribution of the ith optic continnum to C_V.

In order to approach C_V in the anharmonic case we release the quasi-harmonic inference, contradicted by experiments, that a_i=0. It can be shown that C_V corrected for anharmonicity (now called C'_V) is

$$C_v=3nR\sum_{i=1}^{m}C_{vhi}(1-2a_iT)$$

where a_i is the mean value of the measured a_i parameters placed in the ith continuum. If a_i is negative then C_V exceeds the Dulong and Petit limit at HT.

The specific heat at constant pressure and entropy uncorrected for intrinsic anharmonicity are given by

$$C_p=C_V+\alpha^2VKT$$

$$S=S_0+\int_{T_0}^{T}\frac{C_p}{T}dT$$

In the anharmonic case we have

$$C_p'=C_V'+\alpha^2VKT$$

$$S'=S_0+\int_{T_0}^{T}\frac{C_p'}{T}dT$$

S_0 is the quasi-harmonic entropy computed at 298.15 K, where K the bulk modulus α the coefficient of thermal expansion, and V the molar volume.

Anharmonic effects and the α^2KVT term are negligible below 300 K (i.e $C_V'=C_V=C_p=C_p';S=S'$). No anharmonic correction is taken into account for the acoustic modes. Available α, K, V and acoustic velocities values for all the compounds are reported in Table 10.

Results for the GeO_2 Polymorphs

From the available spectroscopic data [Madon et al., submitted manuscript, 1990; this study), a simple density of states can be proposed for each polymorph (Figure 8).

Hexagonal GeO_2. For hexagonal GeO_2, all optically active modes are observed. Therefore, a three-continua model is proposed to take into account the gaps which separate frequency region in which the modes are homogenously distributed (Figure 8). Such a model minimizes the effects of mode dispersion along the Brillouin zone. It also permits the grouping of modes having equivalent anharmonicity in the same continuum. Simpler densities of states also consistent with spectroscopic data (two or three optic continua) have also been tested. They lead to values of C_V (or C_V') similar to within 2% below 300 K and to less than 1% above 500 and up to 1500 K. Correction of C_V (or C_V') to Cp (or C_p') was achieved with two sets of data for α (Table 10); the difference in the α^2KVT term is less than 1% over the 300-1500 K temperature range. A comparison of the calculated C_p and C_p', S and S', and the measured values [King et al., 1958; Counsell and Martin, 1967; Richet, 1989] (C_{pm} and S_m) is presented in Figure 9. The agreement is excellent over the range 0 to 1500 K when anharmonicity is taken into account (C_p' versus C_{pm} values) (Figure 10). The difference between C_{pm} and C_p' is 4% at 50 K, 1% at 200 K, 0.5% at 300 K, and 1.5 % at 1500 K. The same differences are observed for entropy (Figure 9). It must be noticed that C_p calculated with C_V uncorrected for anharmonicity underestimates C_{pm} only above 300 K (8% at 1500 K) (Figure 9).

Tetragonal GeO_2. For tetragonal GeO_2, the simplest model, i.e., with all the optic modes placed in one continuum (Figure 8), is tested. Mean a_i values for each continuum were taken from the measured values of Table 7. This implies that IR and Raman modes in a given continuum have a similar anharmonic behavior although all a_i parameters have not been measured in the case of the IR modes. The corrective term α^2KVT was estimated over the 300-1500 K temperature range with two different sources of data for α (Table 10). These two values lead, to within 1%, to the same values for the corrective term. A much better agreement between C_{pm} and calculated values is observed when anharmonicity is taken into account (C_p' values). The C_V' values are higher than C_V values by 1% at 300 K and 8% at 1500 K. The difference between C_p' and C_{pm} is 5% at 100 K and decreases to less than 1% between 300 and 1500 K (Figure 9). The same differences are observed for entropy (S_m versus S') (Figure 9). Further details are given by Madon et al. [submitted manuscript, 1990]. Such an agreement allows us to use the same modeling for stishovite for which HT calorimetric data are lacking.

Results for the SiO_2 Polymorphs

Kieffer [1979] has shown that her model was able to reproduce reasonably the existing low-temperature (<300 K) calorimetric data of quartz, coesite and stishovite. We use the same approach with slight differences in the density of states and by taking into account mode anharmonicity in the calculations. The proposed density of states for the optic modes are shown in Figure 8.

Quartz. As for hexagonal GeO_2, all the optic modes are active and a four-continuum model is proposed to account for the gaps observed in the mode distribution (Figure 8) and also for the difference in the a_i parameters. The anharmonic correction (C_V' versus C_V values) is of the order of 2% at 300 K and 5% at 800 K (Table 11). The corrective α^2KVT term was calculated with the α values of Ghiorso et al. [1979]. Comparison between computed C_p, C_p',S ,S' , and C_{pm} and S_m [Richet et al., 1982; Hemingway, 1988] are reported in Figure 10 and Table 11. Between 50 and 800 K, C_p' reproduces C_{pm} within ±2%. Above 300 K and up to 800 K, the difference between C_p' and C_{pm} and S' and S_m is less than 1%. Above 500 K, C_p' reproduces the measured values more accurately than C_p. Above 800 K, the model does not reproduce the excess C_p related to the α/β transformation. This is mainly due to the drastic changes observed in the $(\partial\nu_i/\partial T)$ values for certain modes in the vicinity of the transformation temperature [Gervais and Piriou, 1975]. Such changes modify the γ_{iP} values and therefore the a_i parameters. Our model should be more predictive in the transition region by taking into account the variation of a_i with temperature near the transition temperature.

Coesite. For coesite the IR and Raman data shows a continuous group of optically active lines extending from 681 down to 77 cm^{-1}. Two other groups of bands can be isolated between 740-840 and 1036-1226 cm^{-1}. In her model for coesite, Kieffer [1979] has placed 16 modes (corresponding to Si-O stretches) in a single Einstein oscillator at around 1100 cm^{-1} and the remaining 53 optic modes in a single continuum extending from 200 to 700 cm^{-1}.

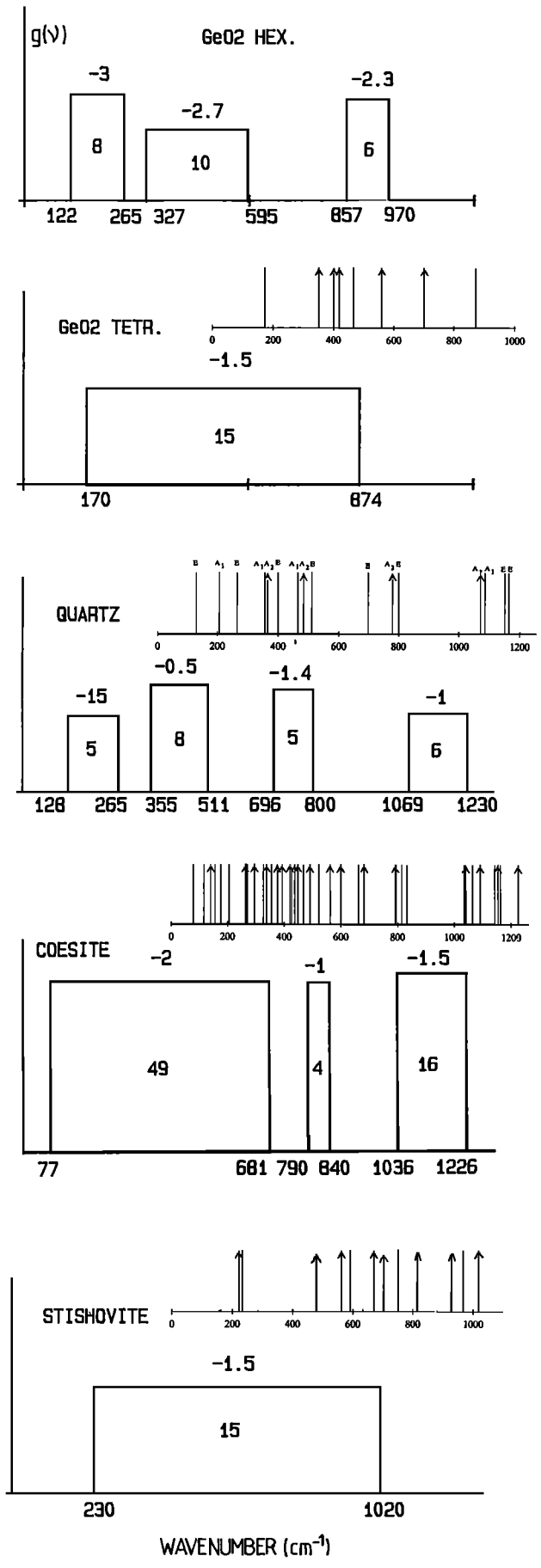

According to our Raman data and those of Hemley [1987] and the available IR data, we propose a slightly different density of states which accounts for the observed gaps in the mode distribution. Anharmonic correction (C_v versus C'_v) is less important than in quartz: 1% at 300 K and 5% at 1500 K (Table 11). The corrective α^2KVT term calculated with different values of $\alpha(T)$ (the dominant parameter in the α^2KVT term) [Skinner, 1966; Duffy and Anderson, 1989; Fei et al., 1990] varies only to within 1%. The computed values of C'_p and S' reproduce the experimental values of Holm et al. [1967] (Figure 10 and Table 11) within 2% between 100 and 300 K. At 300 K, the difference is less than 1%. Anharmonicity leads to a difference between computed C_p and C'_p of 1% at 300 K and 5% at 1500 K. No data of C_{pm} and S_m above 500 K exist. However, Berman [1988] and Fei et al. [1990] proposed polynomnial equations for C_p (300-1500 K), derived from an internally consistent data set which gives C_p values close to within 1-2% to the calculated C'_p values.

Stishovite. To model the density of state of stishovite, we used the simple model developed for tetragonal GeO_2 which appeared to predict successfully both measured C_{pm} and S_m up to 1500 K. Moreover, the similar Raman mode anharmonic behavior of GeO_2 and SiO_2 in the rutile structure supports such a simple model. The density of states for the optical modes is given in Figure 8. Anharmonic correction (C_v versus C'_v) (Figure 10 and Table 11) is 0.5% at 300 K and 3% at 1500 K. The α^2KVT calculated with different values of $\alpha(T)$ [Ito et al., 1974; Endo et al., 1986; Duffy and Anderson, 1989] varies only to within 1%. At low temperatures (<100 K) (Figure 10), the model underestimates S_m and C_{pm} of Holm et al. [1967) by 30% and 20% respectively. At 300 K, S' overestimates S_m by 3% and C'_p underestimates C_{pm} by 3% (Figure 10 and Table 11). Such discrepancies can either be attributed to the sample quality of Holm et al. [1967] or inherent to the too simple density of state used in vibrational modeling. The HT extrapolated C'_p and S' values are given in Figure 10 and Tables 11 and 12. A more precise IR study of synthetic stishovite performed at low and high temperature could probably provide spectroscopic data which could be used to refine the density of state and hence refine the calculated thermodynamic values at low temperatures. However, we believe that the HT values of C'p and S' will not be drastically changed, if the used values of α and K are not strongly different from the values proposed by Duffy and Anderson [1989] and Weidner and Carleton [1977].

Fig. 8. Density of states for the optic modes of the GeO_2 and SiO_2 polymorphs. They have been constructed using the present Raman data (vertical lines) and the IR data (vertical arrows) from Madon et al. [submitted manuscript, 1990] for the GeO_2 polymorphs, Gervais and Piriou [1975] for SiO_2 quartz; Kieffer [1979] for coesite and Hofmeister et al. [1990] for stishovite. The number in each optic continuum refers to the number of modes; the number above gives the mean a_i parameter of the modes placed in this continuum.

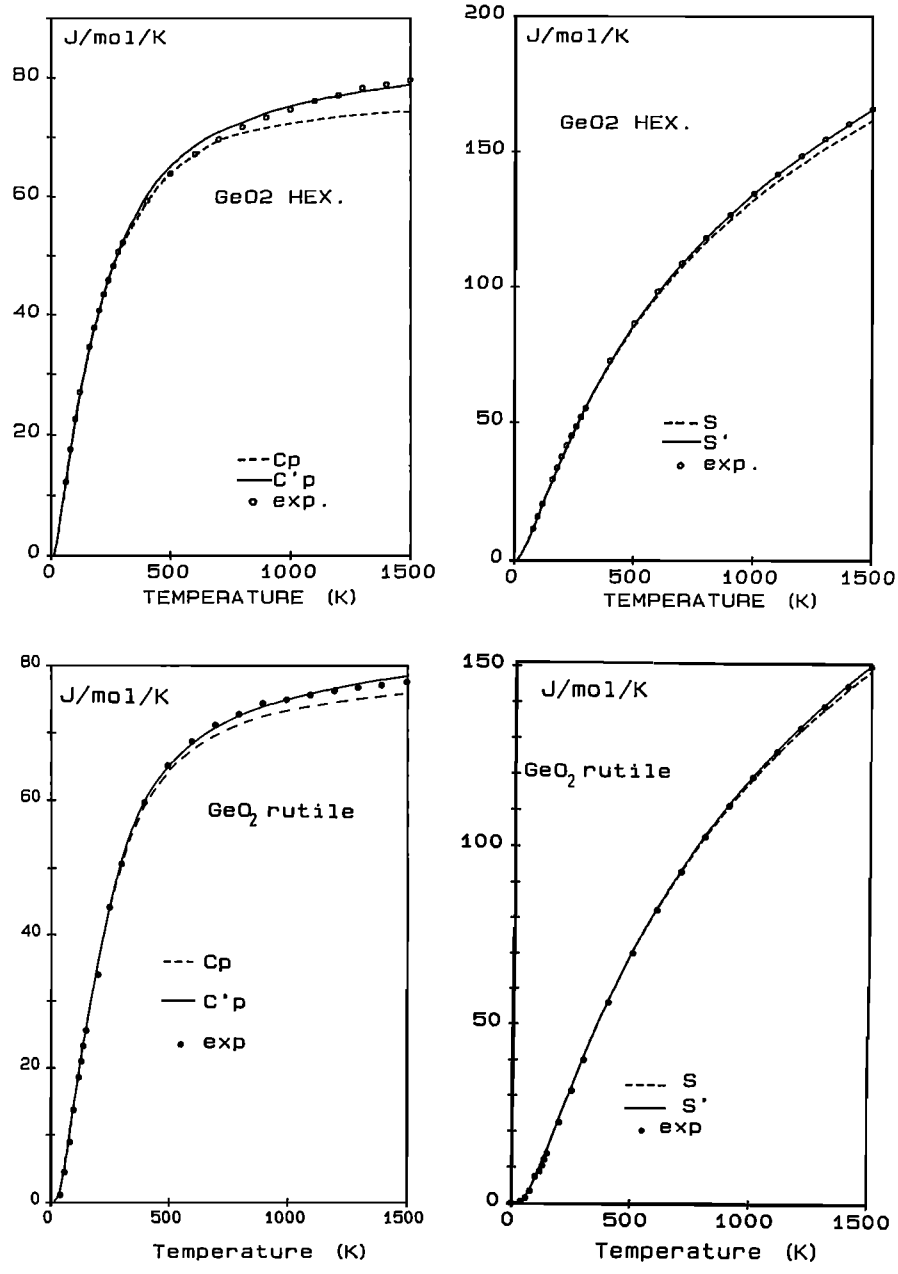

Fig. 9. Thermodynamic properties of the GeO_2 polymorphs [after Madon et al., submitted manuscript, 1990]. Cp (S) and C'p (S') curves represent values calculated with or without anharmonic corrective terms on C_v respectively. Experimental data (points) are from King [1958], Counsell and Martin [1967] and Richet [1989].

Relative thermodynamic properties of the SiO_2 polymorphs: a discussion

Several authors have pointed out the discrepancy among the existing data of the thermodynamic properties of the SiO_2 polymorphs [Weaver et al., 1979; Akaogi and Navrotsky, 1984; Kuskov and Fabrichnaya, 1987; Fei et al., 1990]. For the coesite-stishovite transformation inconsistency is observed between thermochemical data and experimental determinations of the phase boundary. As discussed by Weaver et al. [1979], most of the equilibrium data give lower bound pressures of transition and the derived thermodynamic properties may only be rough estimates. Akaogi and Navrotsky [1984] proposed a data set for coesite and stishovite from high-temperature solution calorimetry. From their data, they concluded that the $\Delta S_{C\text{-}St}(298)$ at the coesite-stishovite transition is 4.2± 1.6 J/mol/K at 298 K and 10.4 J/mol/K at 1500 K. Their results are at variance with the results of Holm et al. (1967) who measured a calorimetric difference $\Delta S_{C\text{-}St}(298)$=12 J/mol/K. The value reported by Akaogi and Navrotsky [1984] for $\Delta S_{C\text{-}St}$ is also rather small in magnitude for a transition involving a large negative

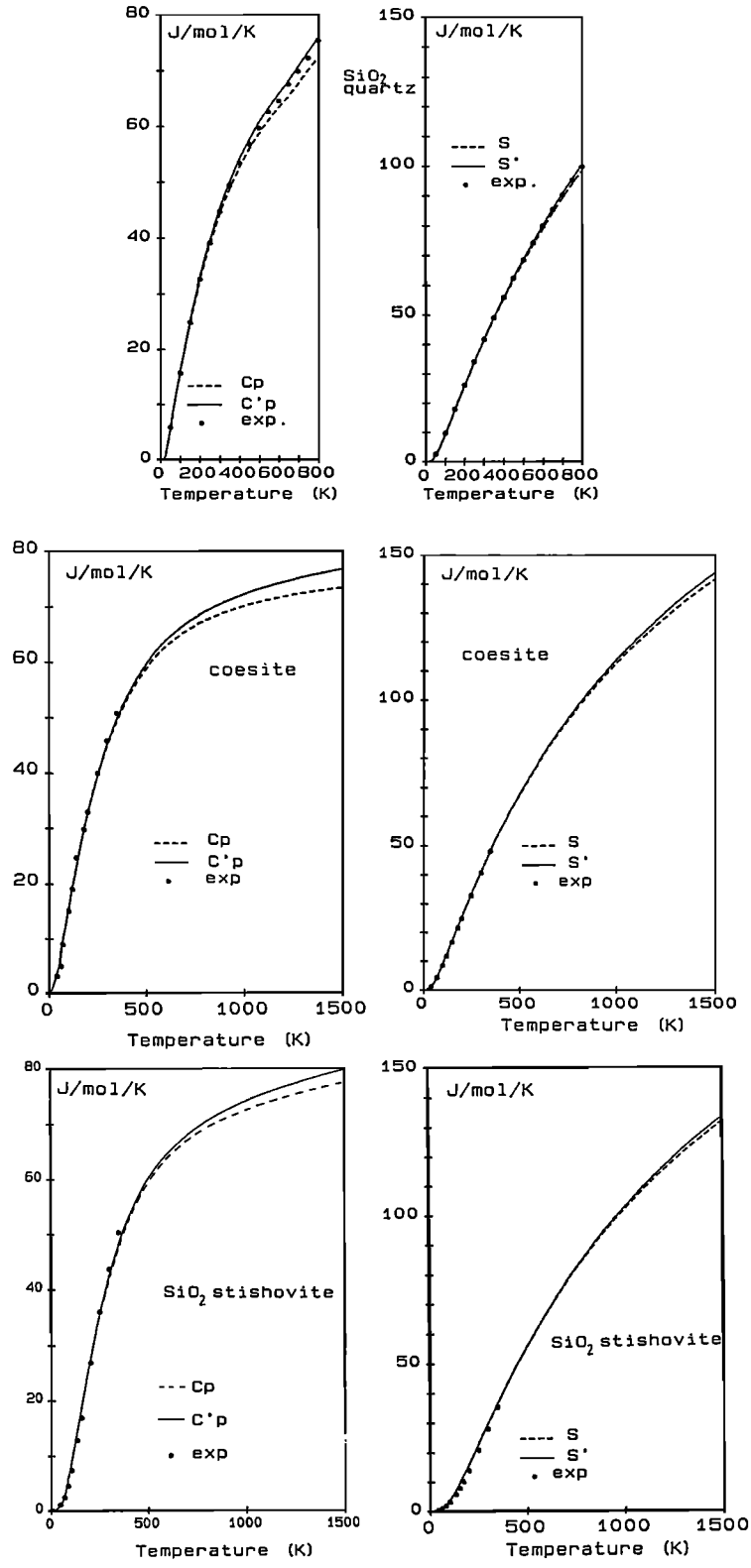

Fig. 10. Thermodynamic properties of the SiO_2 polymorphs. Symbols are the same as in Figure 9.

volume change. It must be noticed that the measurements of Holm et al. [1967] probably provide an upper bound to the actual values of C_p and S for coesite and stishovite, because the sample imperfections quoted by the authors could only lead to Cp and S higher than that of perfect crystals. Hence the calorimetric difference $\Delta S_{C\text{-}St}(298)$ = 12 J/mol/K might represent the magnitude of the lower bound value. Moreover, the HT C_p extrapolations for coesite and stishovite proposed by Akaogi and Navrotsky [1984] show an unsual behavior. In fact the C_p of coesite

TABLE 11. Comparison Between Harmonic and Anharmonic Calculations

T, K	C_V	C'_V	C_p	C'_p	C_{pm}	S	S'	S_m
				Quartz				
50 K	5.72	5.72	5.72	5.72	5.81	2.24	2.24	2.63
100 K	15.98	16.10	15.98	16.10	15.70	9.48	9.52	9.68
300 K	43.89	44.92	44.24	45.26	44.70	41.57	41.68	41.71
500 K	57.94	59.94	58.71	60.71	59.65	67.96	68.71	68.47
700 K	64.76	67.77	67.60	70.71	69.86	89.26	90.74	90.02
800 K	66.79	70.30	72.30	75.81	75.24	98.5	100.81	99.56
				Coesite				
50 K	5.32	5.32	5.32	5.32	4.95	3.35	3.35	2.08
100 K	14.82	14.87	14.82	14.82	15.07	7.97	7.97	8.56
300 K	44.5	45	44.7	45.5	45.6	39.8	39.9	40.66
700 K	65.2	66.8	65.3	66.9		86.9	87.6	
1000 K	69.6	72	69.90	72.3		111	112.5	
1500 K	72.4	76.2	73.1	76.9		139.9	142.6	
				Stishovite				
50 K	1.75	1.75	1.75	1.75	1.46	0.51	0.51	0.74
100 K	9.63	9.63	9.63	9.63	7.16	3.92	3.92	3.2
300 K	43.2	43.4	43.6	43.7	43.2	30.9	31	28.04
700 K	66.0	66.9	67.2	68.1		79	79.5	
1000 K	70.2	71.6	72.3	73.7		103.7	104.7	
1500 K	72.7	74.9	77.7	79.9		134.2	135.7	

It is assumed that $(\partial K/\partial T)$ for all the compounds is -0.02 GPa/K. Values are in J/mol/K.

TABLE 12. Thermodynamic Properties of the SiO_2 Polymorphs

	$Cp=k_0+k_1T^{-0.5}+k_2T^{-2}+k_3T^{-3}$					S_O (T=298.15 K)	
Compound	k_0	k_1	$k_2(10^4)$	$k_3(10^8)$	T° range	Model	Experiment
Quartz	156.71	-2496.47	516.967	-6.57589	270-800 K	41.6	41.44 [a]
Coesite	91.91	-537.344	-299.962	4.70636	298-1500 K	39.3	40.35 [b]
Stishovite	96.89	-678.998	-190.3084	1.92060	298-1500 K	30.6	27.80 [b]

[a]Robie et al. [1982].
[b]Holm et al. [1967].

and stishovite are largely different from those of α-quartz, ß-quartz and cristobalite and even higher than the C_p of liquid SiO_2, and they are in fact responsible for the unsual low value of $\Delta S_{C\text{-}St}(298)$. Finally, it must be noticed that the $\Delta S_{C\text{-}St}$ obtained by Akaogi and Navrotsky [1984] and Kuskov and Fabrichnaya [1987] is 10.4 at 1500 K and 9.1 J/mol/K at 1000 K respectively. These results would be consistent with the room temperature calorimetric data if the C_p of stishovite was close to that of coesite.

The relative C'_p derived from vibrational modeling fitted to polynomnial forms recommanded by Berman and Brown [1985) are given in Table 12. Our model reproduces very well not only the accurately measured thermodynamic properties of α-quartz but also those of coesite and stishovite.

Between 0 and 300 K, both α-quartz and coesite have approximatively the same C'_p and S' values, α-quartz having slightly higher values. The picture is somewhat blurred at higher temperatures by the excess C_p of quartz that preceeds the α-ß transition. Our data confirm that over the range 300-840 K, $\Delta S_{q\text{-}c}$ is positive and hence the equilibrium slope of the α-quartz-coesite boundary is positive. This is in accordance with experimental results which show that down to 573 K, there is no minimum or change of sign of the equilibrium boundary slope [Bohlen and Boettcher, 1982].

Our computed values (C'_p) for coesite are also very close to those provided by the C_p equation given by Berman [1988] and Fei et al. [1990]. The C'_p of stishovite exceeds that of coesite above 500 K but the shapes of the

two curves are quite similar. (Table 12). The C'_p of coesite and stishovite never exceeds that of SiO_2 liquid at HT.

The entropy of stishovite is always smaller than that of quartz or coesite. The ΔS_{C-St} values obtained from our data are quasi-constant over the temperature range 300-1500 K: it varies between 8 and 9 J/mol/K These results are consistent with the ΔS_{C-St} of Holm et al. [1967] at 300 K, ΔS_{C-St} reported by Kuskov and Fabrichnaya [1987] at 1000 K and ΔS_{C-St} of Akaogi and Navrotsky [1984] at 1500 K.

We might therefore conclude that our values of C'p and S' for the three polymorphs are consistent and can be used to compute the equilibrium curve between coesite and stishovite and to compare it to existing experimental equilibrium data.

The slope of the equilibrium curve obtained with our C'p and S' data is of the order of $2x10^{-3}$ GPa/K, in good agreement between 600 and 1500 K with the "best estimate" proposed by Jeanloz and Thompson [1983] and the calculated value of Weaver et al. [1979]. The slope is somewhat lower than than the one of Holm et al. [1967] and higher than that of Akaogi and Navrotsky [1984].

Acknowledgments. This work was financially supported by the French program "DBT (thème: Fluides et Cinétiques)." Contribution INSU n° 206. The coesite and stishovite samples studied in this paper were synthesized by J. Ingrin and F. Guyot in the Stony Brook High Pressure Laboratory, which is jointly supported by the National Science Foundation Division of Earth Sciences (EAR 86-07105) and the State University of New York at Stony Brook. P. Richet (IPG Paris), B. Reynard and A. Chopelas (Max Planck Institut Mainz) are thanked for critical comments of an earlier version of the paper. The careful review of the paper by A. Hofmeister has been appreciated. M. Okuno (Kanazawa University) and I. Minato (JEOL-JAPAN) are greatly thanked for performing the HT Xray measurements of the GeO_2 polymorphs.

References

Anderson, D.L., Temperature and pressure derivatives of elastic constants with application to the mantle, *J. Geophys. Res., 93*, 4688-4700, 1988.

Akaogi, M., and A Navrotsky, The quartz-coesite-stishovite transformations: New calorimetric measurements and calculation of phase diagrams, *Phys. Earth Planet. Inter., 36*, 124-134, 1984.

Akaogi, M., N.L. Ross, P.McMillan, and A Navrotsky, The Mg_2SiO_4 polymorphs (olivine, modified spinel and spinel) - Thermodynamic properties from oxyde melt solution calorimetry, phase relations and models of lattice vibrations, *Am. Mineral., 69*, 499-512, 1984.

Asell, J.F., and M. Nicol, Raman spectrum of α-quartz at high-pressure, *J. Chem. Phys., 49*, 5395-5399, 1968.

Bates, J.B., and A.S. Quist, Polarized Raman spectra of β-quartz, *J. Chem. Phys., 56*, 1528-1533, 1972.

Berge, B., Contribution à l'étude de la phase incommensurable du quartz, Ph.D. Thesis, 110 pp., Université de Grenoble, 1984.

Berman, R.G., Internally-consistent thermodynamic data for minerals in the system Na_2O-K_2O-CaO-MgO-FeO-Fe_2O_3-Al_2O_3-SiO_2-TiO_2-H_2O-CO_2, *J. Petrol., 29*, 445-522, 1988.

Berman R.G., and T.H. Brown, Heat capacity of minerals in the system Na_2O-K_2O-CaO-Mg-FeO-Al_2O_3-SiO_2-TiO_2-H_2O-CO_2 representation estimation and high temperature extrapolation, *Contrib. Mineral. Petrol., 89*, 168-183, 1985.

Bohlen, S.R., and A.L. Boettcher, The quartz-coesite transformation : A precise determination and the effects of other components, *J. Geophys. Res., 87*, 7073-7078, 1982.

Briggs, R.J., and A.K. Ramdas, Piezospectroscopy of the Raman spectrum of α-quartz, *Phys. Rev. B Solid State, 16*, 3815-3826, 1977.

Chopelas, A., Thermal properties of forsterite at mantle pressures derived from vibrational spectroscopy, *Phys. Chem. Miner.,17*, 149-156, 1990.

Counsell, J.F., and J.F. Martin, The entropy of tetragonal germanium dioxyde, *J. Chem. Soc.A*, 560-561, 1967.

Dayal, B., The vibration spectrum of rutile, *Proc. Indian Acad. Sci., A32*, 304-312, 1950.

Dean, K.J., W.F. Sherman, and G.R. Wilkinson, Temperature and pressure dependence of the Raman active modes of vibration of α-quartz, *Spectrochim. Acta, 38A*, 1105-1108, 1982.

Dietrich, P., and J. Arndt, Effects of pressure and temperature on the physical behaviour of mantle-relevant olivine, orthopyroxene and garnet: II. Infrared absorption and Grüneisen parameters, in *High pressure Researches in Geoscience,* edited by W. Schreyer, pp. 307-309, E. Schweizerbart'sche, Stuttgart Germany , 1982.

Duffy, T., and D.L. Anderson, Seismic velocities in mantle minerals and the mineralogy of the upper mantle, *J. Geophys. Res., 94*, 1895-1912, 1989.

Endo, S., T. Akai, Y. Akahama, M. Wakatsuki, T. Nakamura, Y. Tomii, K. Kato, Y. Ito, and M. Tokonami, High temperature X-ray study of single crystal stishovite synthetized with Li_2WO_4 flux, *Phys. Chem. Miner., 13*, 146-151, 1986.

Fei, Y., S.K Saxena, and A. Navrotsky, Internally consistent thermodynamic data and equilibrium phase relations for compounds in the system MgO-SiO_2 system at high pressure and high temperature, *J. Geophys. Res., 95*, 6915-6928, 1990.

Gervais F., and Piriou B., Temperature dependence of transverse and longitudinal optic modes in the α and ß phases of quartz, *Phys. Rev B. Solid State, 11*, 3944-3950, 1975.

Ghiorso, M.S., I.S.E. Carmichael, and L.K. Moret, Inverted high-temperature quartz., *Contrib. Mineral. Petrol., 68*, 307-323, 1979.

Gillet, Ph., J.M. Malezieux, and M.C. Dhamelincourt, MicroRaman multichannel spectroscopy up to 2.5 GPa using a sapphire anvil cell: Experimental set-up and some applications, *Bull. Mineral., 111*, 1-15, 1988.

Gillet, Ph., F. Guyot, and J.M. Malezieux, High pressure and high temperature Raman spectroscopy of Ca_2GeO_4: Some insights on anharmonicity, *Phys. Earth Planet. Inter.*, *58*, 141-154, 1989a.

Gillet, Ph., F. Guyot, and G. Fiquet, Gruneisen parameter and anharmonic behaviour of olivine type compounds, EUG V, Terra Abst., *229*, 1989b.

Hemingway, B.S., Quartz : heat capacities from 340 to 1000 K and revised values for the thermodynamic properties, *Am. Mineral.*, *72*, 273-279, 1987.

Hemley, R.J., Pressure dependence of Raman spectra of SiO_2 polymorphs: α-quartz, coesite et stishovite, in *High-Pressure Research in Mineral Physics*, edited by N.H. Manghnani and Y. Syono, pp. 347-359, Terra Scientific-AGU, Washington DC USA, 1987.

Hemley, R.J., H.K Mao, and E.C.T. Chao, Raman spectrum of natural and synthetic stishovite, *Phys. Chem. Minerals.*, *13*, 285-290, 1986.

Hofmeister, A.M., Single-crystal absorption and reflection infrared spectroscopy of forsterite and fayalite, *Phys. Chem. Miner.*, *14*, 499-513, 1987.

Hofmeister, A.M, J. Xu, and J. Akimoto, Infrared spectroscopy of synthetic and natural stishovite, *Am. Mineral., in press*, 1990

Holm, J.L., O.J. Kleppa, and E.F. Westrum Jr., Thermodynamics of polymorphic in silica thermal properties from 5 to 1070°K and pressure-temperature stability fields for coesite and stishovite, *Geochim. Cosmochim. Acta*, *31*, 2289-2307, 1967.

Ito, H., K. Kawada, and S.I. Akimoto, Thermal expansion of stishovite., *Phys. Earth Planet. Inter.*, *8*, 277-281, 1974.

Jeanloz, R., and M. Roufosse, Anharmonic properties: Ionic model of the effects of compression and coordination change, *J. Geophys. Res.*, *87*, 10763-10772, 1982.

Jeanloz, R., and A.B. Thompson, Phase transitions and mantle discontinuities, *Rev. Geophys.*, *21*, 51-74, 1983.

Kieffer, S.W., Thermodynamics and lattice vibrations of minerals,3, Lattice dynamics and an approximation for minerals with application to simple substances and framework silicates, *Rev. Geophys.*, *17*, 35-59, 1979.

King, E.G., Low-temperature heat capacities and entropies at 298.15 K of some oxydes of gallium, germanium, molybdenum and niobium., *J. Am. Chem. Soc.*, *80*, 1799-1800, 1958.

Kuskov, O.L., and O.B. Fabrichnaya, The SiO_2 polymorphs: The equations of state and thermodynamic properties of phase transformations, *Phys. Chem. Miner.*, *14*, 58-66, 1987.

Lieberman, R., Elastic properties of polycrystalline SnO_2 and GeO_2: Comparison with rutile data, *Phys. Earth Planet. Inter.*, *7*, 461-465, 1973.

Levien, L., and C.T. Prewitt , High-pressure crystal structure and compressibility of coesite, *Am. Mineral.*, *66*, 324-333, 1981.

Mammone, J.F., and H.K. Sharma, Pressure and temperature dependence of the Raman spectra of rutile-structure oxydes, *Year Book Carnegie Inst. Washington 1979*, 369-373.

McMillan, P.F., and A.C. Hess, Ab-initio valence force field calculations for quartz, *Phys. Chem. Miner.*, *17*, 97-107,1990.

McSkimmin, H.J., P. Andreatch, and R.N. Thurston, Elastic moduli of quartz versus hydrostatic pressure at 25°C and -195.8°C, *J. Appl. Phys.*, *36*, 1624-1632, 1965.

Murthy, K.M., Thermal expansion of vitreous and crystalline germania, *J. Am. Ceram. Soc.*, *45*, 616-617, 1962.

Nicol, M., J.M. Besson, and B. Velde, Raman spectra and structure of stishovite, in *High Pressure Science and Tecnology-Proceedings VIIth AIRAPT Conference*, edited by B. Vodar and P. Marteau, pp. 891-893, Pergamon, New York, 1980.

Peercy, P.S., and B. Morosin, Pressure and temperature dependence of the Raman-active phonons in SnO_2, *Phys. Rev. B Solid State*, *7*, 2779-2786, 1973.

Rao, K.V.K., S.V.N. Naidu, and L. Iyengar L., Thermal expansion of rutile type GeO_2, *J. Am. Ceram. Soc.*, *51*, 467-468, 1968.

Richet, P., Superheating, melting and vitrification through decompression of high-pressure minerals, *Nature*, *331*, 56-58, 1988.

Richet, P., GeO_2 vs SiO_2: Glass transitions and thermodynamic properties of polymorphs, *Phys. Chem. Miner.*, *17*, 79-88, 1989.

Richet, P., Y. Bottinga, L. Denielou, J.P. Petitet, and C. Tequi, Thermodynamic properties of quartz, cristobalite and amorphous SiO_2: Drop calorimetry measurements between 1000 and 1800 K and a review from 0 to 2000 K, *Geochim. Cosmochim. Acta*, *46*, 2639-2658, 1982.

Robie R.A., B.S. Hemingway, and J.R. Fisher, Thermodynamic properties of minerals, *U.S. Geol. Surv. Bull.*, 1452 pp., 1978.

Scott , J.F., Raman spectra of GeO_2 quartz, *Phys. Rev. B Solid State*, *1*, 3488-3493, 1970.

Scott, J.F., and S.P.S. Porto, Longitudinal and transverse optical lattice vibrations in quartz, *Phys. Rev. B Solid State*, *161*, 903-910, 1967.

Shapiro, S.M., D.C. O'Shea, and H.Z. Cummins, Raman scattering study of the alpha-beta phase transition in quartz, *Phys. Rev. Lett.*, *19*, 361-364, 1967.

Sharma, S.K., Applications of advanced Raman spectroscopic techniques in Earth Sciences, in *Raman Spectroscopy: Sixty Years on Vibrational Spectra and Structure*, vol. 17B, edited by H.D. Bist, J.R. Durig, and J.F. Sullivan, pp. 513-568, Elsevier Science New York, 1989.

Sharma, S.K., J.F. Mammone, and M.F. Nicol, Raman investigations of ring configurations in vitreous silica, *Nature*, *292*, 140-141, 1981.

Skinner, B.J., Thermal expansion, in *Handbook of Physical Constants*, edited by S.P. Clark, *Memoir Geol. Soc. America* , *97*, 75-96, 1966.

Skinner, B.J., and J.J. Fahley, Observations on the inversion of stishovite to silica glass, *J. Geophys. Res.*, *68*, 5595-5604, 1963.

Soga, N., Sound velocities of some germanate compounds and its relation to the law of corresponding states, *J. Geophys. Res.*, *76*, 3983-3989.

Striefler, M.E., and G.R. Barsch, Elastic and optical properties of stishovite, *J. Geophys. Res., 81*, 2453-2446, 1976.

Suito, K., Phase relations of pure Mg_2SiO_4 up to 200 kbar, in *High pressure research: Applications in Geophysics.*, edited by M.H. Manghnani, and S. Akimoto, pp. 255-266, Academic San Diego Calif., 1977.

Sumino, Y., and O.L Anderson., Elastic constants of minerals, in *Handbook of Physical Properties of Rocks*, vol. 3, edited by R.S. Carmichael, pp. 39-138, CRC Press,, 1982.

Weaver, J.C., D.W. Chipman, and T. Takahashi, Comparison between thermochemical and phase stability data for the quartz-coesite-stishovite transformations, *Am. Mineral., 64*, 604-614, 1979.

Weidner, D.J., and H.R. Carleton, Elasticity of coesite, *J. Geophys. Res., 82*, 1334-1346, 1977.

Weidner, D.J., J.D. Bass, A.E. Ringwood, and W. Sinclair, The single-crystal elastic moduli of stishovite, *J. Geophys. Res., 87*, 4740-4746, 1982.

Werner-Kieffer, S., Shock processes in porous quartzite: Transmission electron microscope observations and theory, *Tectonophysics, 59*, 41-93, 1976.

Zallen, R., and M.L. Slade, Influence of pressure and temperature in molecular chalcogenides: Crystalline As_4S_4 and S_4N_4, *Phys. Rev. B Condens. Matter, 18*, 5775-5798, 1978.

Ph. Gillet and A. Le Cléac'h, Laboratoire de Minéralogie Physique, CAESS, Université de Rennes I, 35042 Rennes, France.

M. Madon, Département des Géomatériaux, Institut de Physique du Globe Paris, 4 place Jussieu, 75252 Paris, France.

(Received February 6,1990;
revised July 30,1990;
accepted August 7,1990.)